ACS APPLIED BIO MATERIALS

www.acsabm.org Article

Identifying Factors that Determine Effectiveness of Delivery Agents in Biolistic Delivery Using a Library of Amine-Containing Molecules

Kyle J. Miller, Connor Thorpe, Alan L. Eggenberger, Keunsub Lee, Minjeong Kang, Fei Liu, Kan Wang,* and Shan Jiang*

Cite This: https://doi.org/10.1021/acsabm.2c00689 Read Online

ACCESS | Metrics & More | Article Recommendations | Supporting Information

ABSTRACT: Biolistic transfection is a popular and versatile tool for plant transformation. A key step in the biolistic process is the binding of DNA to the heavy microprojectile using a delivery agent, usually a positively charged molecule containing amine groups. Currently, the choice of the commercial delivery agent is mostly limited to spermidine. In addition, the detailed delivery mechanism has not been reported. To help broaden the selection of the delivery agent and reveal the fundamental mechanisms that lead to high delivery performance, a library of amine-containing molecules was investigated. A double-barrel biolistic delivery device was utilized for testing hundreds of samples with much-improved consistency. The performance was evaluated on onion epidermis. The binding and release of DNA were measured *via* direct high-performance liquid chromatography analysis. This study shows that the overwhelming majority of the amine library performed at the same level as spermidine. To further interpret these results, correlations were performed with thousands of molecular descriptors generated by chemical modeling. It was discovered that the overall charge is most likely the key factor to a successful binding and delivery. Furthermore, even after increasing the amount of the DNA concentration 50-fold to stress the binding capacity of the molecules, the amines in the library continued to deliver at a near identical level while binding all the DNA. The increased DNA was also demonstrated with a Cas9 editing test that required a large amount of DNA to be delivered, and the result was consistent with the previously determined amine performance. This study greatly expands the delivery agent selection for biolistic delivery, allowing alternatives to a commercial reagent that are more shelf-stable and cheaper. The library also offers an approach to investigate more challenging delivery of protein and CRISPR-Cas *via* the biolistic process in the future.

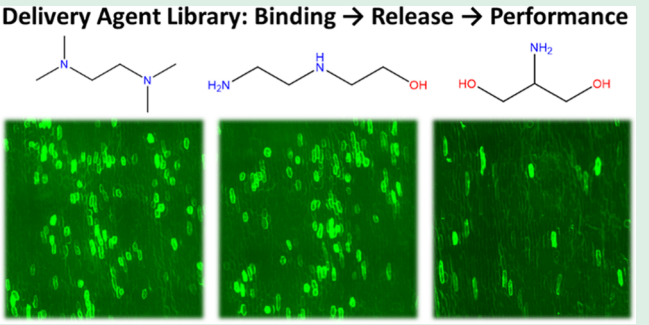

KEYWORDS: *DNA delivery, DNA−particle precipitation, gene editing, gene gun, particle bombardment, QSAR*

1. INTRODUCTION

The genomic editing of plants is a key technology for meeting global demand for food, pharmaceuticals, and sustainable energy, with genetic enhancement improving crop yields, nutritional content, and the development of sustainable biofuels.[1−5] Several routes have emerged to genetically modify plant systems, such as gene transfer *via* *Agrobacterium*-mediated plant transformation or chemical-induced transfection in protoplasts. The gene gun, or biolistic method, is another tool used to deliver DNA into plant cells by binding them to a heavy metal particle and launching it at high speeds to penetrate the cell wall. It has been used in every facet of the gene delivery industry since its initial development in 1987.[6,7] The main advantage of biolistic bombardment is its versatility. In contrast to *Agrobacterium*-mediated transformation or protoplast transfection, biolistics works with virtually any plant species and has the potential to deliver alternative payloads such as viruses[8] or ribonucleoproteins (RNPs) such as the CRISPR-Cas9 system.[9]

Since its inception,[10] the protocol for biolistic transfection has remained mostly unchanged. A heavy metal particle, such as gold or tungsten, is co-precipitated with DNA using a cationic molecule and a salt such as calcium chloride to form a DNA−particle complex. This complex is then propelled by a gas burst in a biolistic device with enough force to break through the cell wall. Once the DNA−gold complex is in the cell, the DNA is released, allowing it to be expressed inside the cell nucleus. Of these steps of binding, bombardment, and release, significant focus has been applied to the bombardment stage, with optimized protocols now available for a variety of

Received: August 7, 2022
Accepted: September 20, 2022

plant species and even extending the application into varieties of animal cells.[7,11−13]

However, less attention has been given to the impact of the binding and release of the DNA from the gold particles, a vital step in the process. The critical factor for both these steps is the cationic molecules whose positively charged amine groups facilitate the binding between the negatively charged gold and DNA, likely through electrostatic interactions. While many different molecules have amine groups, spermidine is near-universally used for biolistic protocols.[6,7,10−18] To the best of our knowledge, the formation of the DNA−gold complex has never been thoroughly investigated, leaving it relatively unknown what factors could lead to its improvement.

This work investigates alternatives to spermidine by testing a library of similar amine structures. Libraries have seen great utility in improving gene and drug formulations to animal cells.[19−21] The library used in this work was generated by incorporating commercially available amines, with the foremost requirement being that they contain at least one amine functional group. By testing a variety of structures, it becomes possible to understand the cause-and-effect relationship between molecular properties and the biolistic DNA delivery. While some amines are more expensive, it is worth noting as well that a large portion of the library is significantly cheaper than the standard spermidine.

However, biolistic bombardments often suffer from significant sample-to-sample variation that prohibits large-scale comparisons. To overcome this, we used the double-barrel method discussed in the previous work[22] to enable a high-throughput, reliable analysis of biolistic results. The double-barrel modification to the gene gun allows for the parallel bombardment of a single tissue sample. This allows normalization of the bombardment results, which significantly reduces sample-to-sample variation and the number of bombardments required to establish reliable data of the performance. In combination with a customized application of the CellProfiler software,[23] these tools enabled the rapid testing of the entirety of the library, measuring the expression of a green fluorescent protein (GFP) gene in onion epidermis *via* imaging and image analysis.

To further understand the delivery mechanism, high-performance liquid chromatography (HPLC) analysis was carried out to measure the binding and release of DNA. By examining supernatants taken during simulated binding and release steps, unbound DNA was quantified with HPLC to reduce or eliminate background absorbance from other molecules in the mixture. In addition, to understand how different chemical structures influence the delivery results, the delivery efficiency of the library structures was correlated with their chemical descriptors. The descriptor values are generated using the Online Chemical Database modeling environment and describe various properties. Descriptors can be as simple and direct as the number of atoms of a certain element or functional group or as complex as an indicator for solubility or a predicted melting point.[24−26] Combining the library with the descriptor database offers a way to identify the underlying structures and mechanisms that determine the delivery performance.

2. EXPERIMENTAL SECTION

2.1. Materials. The amine library is made up of 50+ molecules whose names were arbitrarily assigned using a naming convention of letter + number (*e.g.*, N13, X30, NS1). All amines were purchased from Millipore Sigma (Burlington, MA, USA) or Thermo Fisher Scientific (Waltham, MA, USA) at purities at or above 95% (Supporting Table S1 lists structure names, while the structures are shown in Supporting Figure S1). Gaps in the numbering are either because of redundant structures or because of solubility issues with the molecule once acquired that resulted in subsequent removal from the library.

The standard Bio-Rad PDS-1000/He gene gun (Bio-Rad Life Science, Hercules, CA, USA) was used with 0.6 μm gold particles and stopping screens purchased from the same company. Macrocarriers and 650 psi rupture discs were purchased from Analytical Scientific Instruments (Richmond, CA, USA). The reporter plasmid pLMNC95[27] contains an endoplasmic reticulum-localized GFP (ER-GFP) cassette. The plasmids pKL2187[22] and pTF6005[28] were used for the Cas9 studies. The double barrel was used with permission from Kale and Tyler's original design,[29,30] and later, a modified version was made *via* 3D printing. Finally, white onions (*Allium cepa*) were obtained from a local grocery store. Sections of epidermis >2 × 2 cm were removed from the inner surface of the onion scales before shooting and placed onto agar plates containing 0.7% Difco Bacto Agar made in 0.5 mM 2-(*N*-morpholino) ethanesulfonic acid (MES) buffer (pH 5.6).

2.2. Bombardment. The bombardment was performed using the double-barrel protocol described in the previous work.[22] First, the DNA−gold complex was prepared. The protocol for eight bombardments involved mixing 25 μL of gold particles at 12 mg/mL with 10 μL of plasmid pLMNC95 at 20 ng/μL, followed by 25 μL of 2.5 M $CaCl_2$ and 10 μL of 0.1 M spermidine or amine from the library. After mixing for 30 s, the tubes were centrifuged using the pulse function for roughly 15 s, and the supernatant was removed. The particles were briefly resuspended in 70 μL of 70% ethanol and centrifuged again. After removing the final supernatant, the particles were resuspended again in 50 μL of 40% ethanol. Aliquots of 6 μL of the suspension were deposited onto a macrocarrier and vacuum-dried. A series of images showing the particle condition in different states is shown as Supporting Figure S2. This leads to a per-bombardment equivalent of 36 μg of gold, 24 ng of DNA, 3 μL of $CaCl_2$, and 1.2 μL of amine (0.1 M) at the given concentrations.

To use the double barrel, macrocarriers were marked on the helium-facing side to symmetrically place the aliquots of the DNA−gold complex. Typically, a sample using spermidine was prepared in parallel with one using a library amine. The double-barrel attachment replaced the stopping screen holder and spacer rings found in the stock PDS-1000/He. The macrocarrier was aligned with the openings, and the onion epidermis was bombarded at 650 psi using the 9 cm target distance.

After bombardment, plates were wrapped in parafilm and incubated at room temperature for at least 24 h before imaging and analysis. Images were taken using a Leica DMi8 inverted microscope with an automated stage and digital camera. Low magnification was used in conjunction with the tilescan feature to merge multiple images into a mosaic. Fluorescence images were captured with an FITC filter set (excitation: 460−500 nm; emission: 512−542 nm) or a Texas Red filter set (excitation: 542−582 nm; emission: 604−644 nm). Cell analysis was done using CellProfiler 3.1.9, an updated version for Windows on a Windows 10 PC. CellProfiler is a free open-source software platform designed to enable easy quantification of biological images.[23] The analysis pipeline was built using basic CellProfiler options, with validation described in previous work.[22] The pipeline is described in the Supporting Information.

2.3. HPLC Analysis. Binding and release tests were conducted *via* HPLC analysis. The biolistic shot preparation described above was repeated, and the first supernatant, containing unbound DNA, was saved for analysis by adding it to a vial and filling it to the minimum testable volume (700 μL) with 20 mM Tris-HCl buffer (pH 8.0). The biolistic shot preparation was continued up to the final step, but instead of resuspending the gold−DNA complexes in 40% ethanol for loading onto the microcarrier, they were resuspended in 100 μL of 4 mM MES pH 5.6 20 mM KCl for DNA release. After 1 h with occasional mixing, the tubes were centrifuged, and the supernatant

https://doi.org/10.1021/acsabm.2c00689
ACS Appl. Bio Mater. XXXX, XXX, XXX−XXX

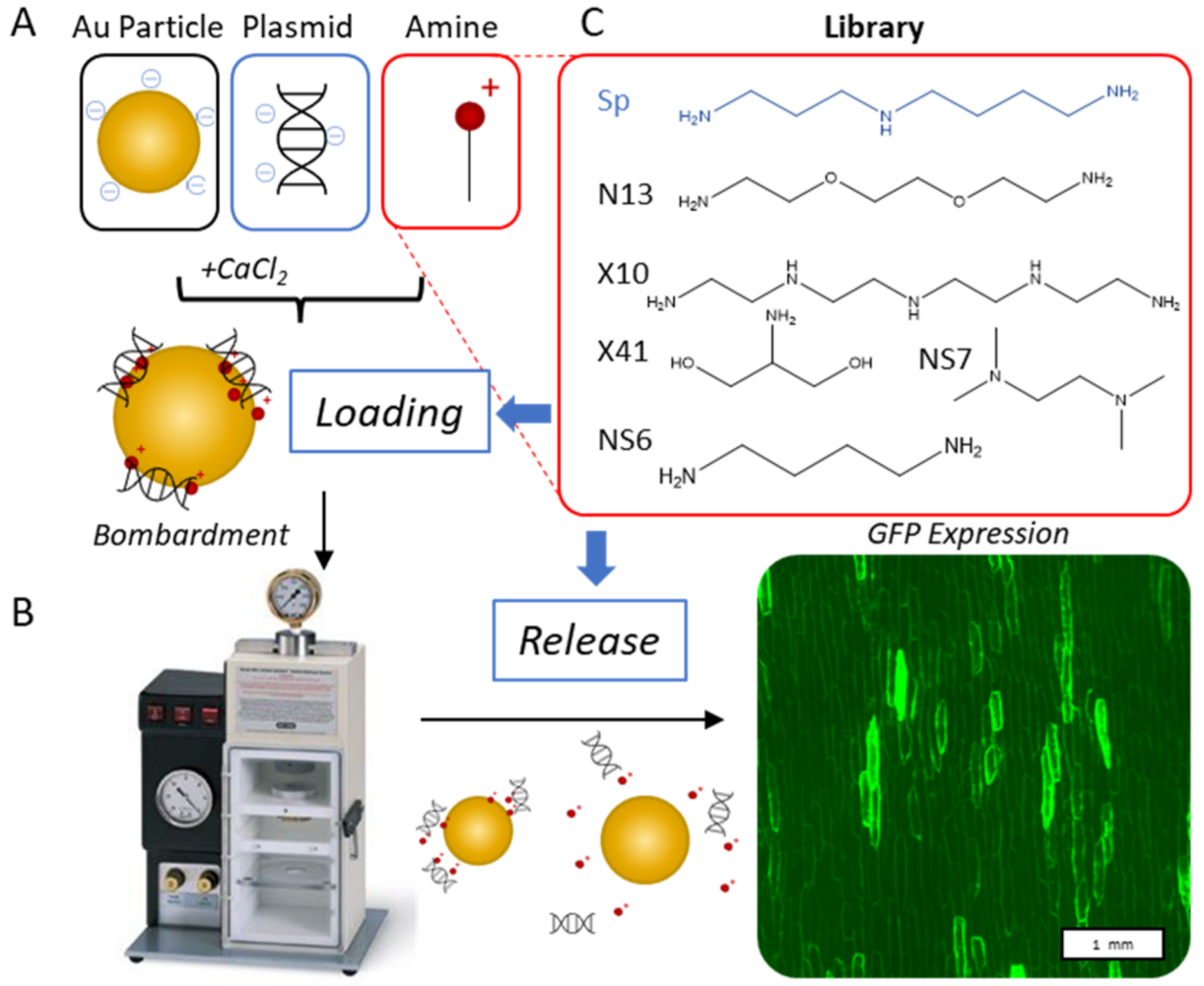

Figure 1. Schematic diagram showing the role the amine plays in the precipitation of DNA onto a biolistic particle. (A) Standard biolistic protocol calls for a mixture of micron-sized gold particles, plasmid DNA, and an amine, with the respective charges shown. When a strong salt like $CaCl_2$ is added, the components begin to aggregate. Because of the slight negative charge of the metallic surface and the DNA, a positively charged molecule like an amine is required for the DNA to aggregate with the gold and form a complex that can survive bombardment. (B) Particles are then bombarded using a gene gun such as the PDS-1000/He. Once inside the cell, the aggregate breaks apart due to the lower salt concentration and the pH drop, allowing the DNA to be expressed, such as the fluorescent cells in the picture. (C) This study investigates the role of the amine in the delivery of the DNA by comparing the performance of an amine library (representative subset shown) to spermidine, the long-standing standard used (colored blue). The scale bar is 1 mm.

was added to a vial that was then filled up with 20 mM Tris buffer to the minimum testable volume (700 μL). The vials were then processed in the HPLC system, extracting 20 μL of the sample and testing for absorbance primarily at the 260 nm wavelength. In each batch, peaks identified on the 260 nm absorbance curve were compared to a known quantity of DNA. Each sample was tested twice, and data were discarded if peaks were not in agreement with each other.

The instrument used for HPLC analysis was an LC-20A liquid chromatograph (Shimadzu, Japan) consisting of two LC-20AT pumps, an SPD-20 UV/vis detector, and a DGU-$20A_3$ degasser. The flow protocol used ion exchange using 20 mM Tris-HCl buffer (pH 8.0), which gradually shifted up to 1 M NaCl concentration. DNA was separated on a TSKgel DEAE-NPR anion-exchange column (35 mm × 4.6 mm id, 2.5 μm) with a TSKgel DEAE-NPR guard column (5 mm × 4.6 mm id, 5 μm), both from Tosoh Bioscience (King of Prussia, PA). The column was equilibrated with a mobile phase composition of 50:50 20 mM Tris-HCl pH 8.0 and 20 mM Tris-HCl, 1 M NaCl, pH 8.0. The gradient increased to 100% 20 mM Tris-HCl, 1 M NaCl, pH 8.0 over 10 min with a flow rate of 0.5 mL min^{-1}.

2.4. Descriptor Generation. Descriptors were generated *via* the Online Chemical Database with the modeling environment (ochem.eu).[31] Molecules were uploaded as a .sdf file, standardized using CDK standardizer, which neutralized and removed salts. The models selected to generate descriptors were OEState, AlogPS, alvaDesc v.2.0.4, Dragon v. 7, CDK 2.7.1, Chemaxon (pH range = all), and "Inductive" descriptors.

2.5. Statistical Analysis. Data were handled, and figures were made in Origin (OriginLab) or Excel (Microsoft). Data presented with error bars represent at least 5 replicates, with the error bar indicating one standard deviation in either direction, while data without error bars indicate data from an individual experiment. Significance in this work refers to a *p*-value of less than 0.05 using a Student's *t*-test assuming independent samples. R^2 values were generated in Excel using the data from Figure 3a as the dependent variable and descriptors as the independent variable.

3. RESULTS AND DISCUSSION

3.1. Library Testing. The long-standing protocol for biolistic delivery is to mix the negatively charged DNA and gold with the cationic molecule spermidine and a concentrated

https://doi.org/10.1021/acsabm.2c00689
ACS Appl. Bio Mater. XXXX, XXX, XXX−XXX

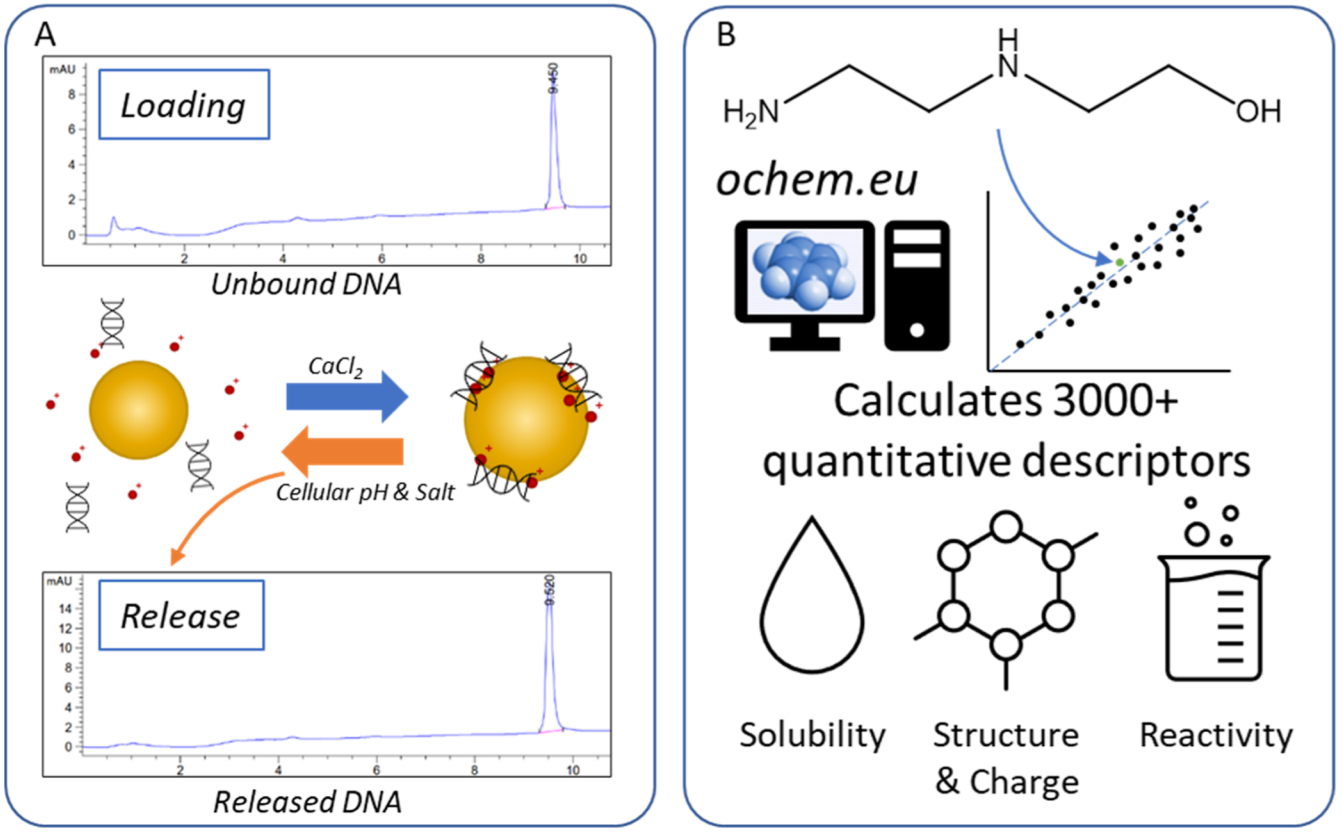

Figure 2. Schematic diagrams showing the role the amine plays in the precipitation of DNA onto a biolistic particle. (A) HPLC was used to supplement biolistic data and better analyze the behavior of the complex formation. After standard complex formation, the aliquot was extracted and analyzed in order to quantify the unbound DNA remaining in the solution. Then, the same particles were resuspended in a solution mimicking the cellular environment (pH = 6.0 through MES buffer and KCl) and released DNA was analyzed similarly. (B) To improve understanding, the library molecules were quantified as molecular descriptors. Using the online modeling database ochem.eu,[31] the molecules were broken down into 3000+ molecular descriptors, which predict features ranging from solubility to charge to molecular topology.

salt such as $CaCl_2$ (Figure 1A). The salt shields charge, reducing electrostatic repulsion and leading to rapid precipitation of the DNA and gold. Precipitation occurs without the spermidine, but DNA was not bound to the gold, leading to unsuccessful DNA delivery (Supporting Figure S3). However, with spermidine in the mixture, they formed a complex that persisted through two washing steps, drying, and a high-speed acceleration, only to release DNA in the cell (Figure 1B).

In this work, we compared spermidine to a library of similar molecules (Supporting Table S1 and Supporting Figure S1) to better understand the structure−property relationship in the DNA−gold complex formation. The amine functional groups on spermidine were thought to be the likely factor in the proper complex formation, so all structures contained at least one amine functional group. The factors that were varied included the number of amines, their relative positions in the structure, the bonding state of the amine (primary, secondary, tertiary), total molecular weight (50−250 g/mol), and the addition of some other functional groups such as alcohols and ethers. A subset of the library is shown in Figure 1C. Amine-containing molecules (referred to as amines hereafter) were eventually excluded if their water solubility was below or near the 0.1 M concentration used.

The amine library was directly tested using a previously reported double-barrel and imaging system,[22] which enabled high-throughput biological testing (Supporting Figure S4). Onion epidermis was bombarded with a plasmid encoding GFP, followed by imaging to collect the transient expression data. With the double-barrel protocol, a single piece of tissue was divided in half and bombarded in parallel with a spermidine control as well as the test sample. After an incubation period of 24−48 h, the samples were scanned and analyzed *via* the CellProfiler software.[23] The numbers of transfected cells on the spermidine and library amine halves were compared by dividing the number of transfected cells on the test amine side by the cells on the spermidine side. This value was termed the performance ratio and represents the ability of an amine to deliver DNA, normalized by the spermidine internal control; a value of 1 indicates that the amine performed at the same level as the spermidine sample, while higher numbers indicate a higher number of cells expressing GFP and low numbers indicate the opposite. Each amine received at least 10 bombardments, with some receiving more than 20 to reduce the variance. Onion epidermal tissues that appeared damaged or otherwise compromised were discarded. Toxicity was briefly investigated using fluorescein diacetate/propidium iodine viability assay. We qualitatively found no difference between several randomly selected amines and spermidine (Supporting Figure S5).

To further understand the delivery mechanism, HPLC was utilized to directly quantify the amount of DNA bound to the gold particles by the different amines as well as the amount released afterward (Figure 2A). During the initial mixing and

https://doi.org/10.1021/acsabm.2c00689
ACS Appl. Bio Mater. XXXX, XXX, XXX−XXX

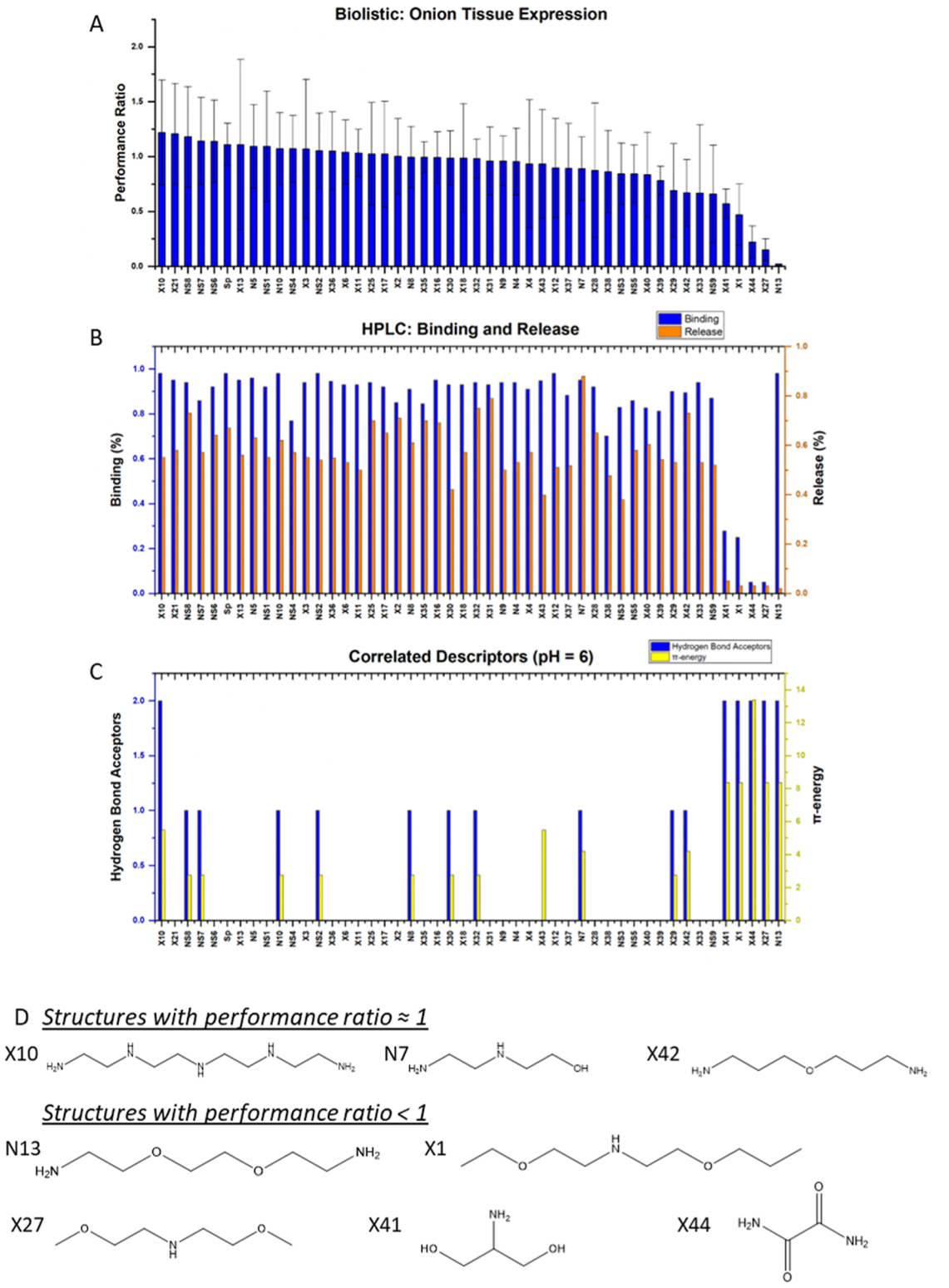

Figure 3. Library testing results. (A) For each amine, between 10 and 30 onion tissue samples were bombarded with the dual-barrel testing method using spermidine as a control. The average performance ratio is shown of viable samples. (B) DNA concentration was tested using HPLC to determine binding and release behavior for each amine. The binding sample was generated by measuring the supernatant after precipitation, while the release followed 1 h of precipitate resuspension in a simulated cellular environment. (C) Calculated value for most negative local charge for each amine. (D) Structure of amines with the largest negative charge value.

precipitation, the supernatant, which is normally discarded, was kept and analyzed for unbound DNA. When particles were resuspended before deposition onto the macrocarrier, they were instead placed in a release solution of 4 mM MES (pH 5.6) and 20 mM KCl for 1 h, with the supernatant extracted and analyzed for released DNA.

Additionally, quantitative structure−activity relationship (QSAR) molecular descriptors were utilized to identify trends

https://doi.org/10.1021/acsabm.2c00689
ACS Appl. Bio Mater. XXXX, XXX, XXX−XXX

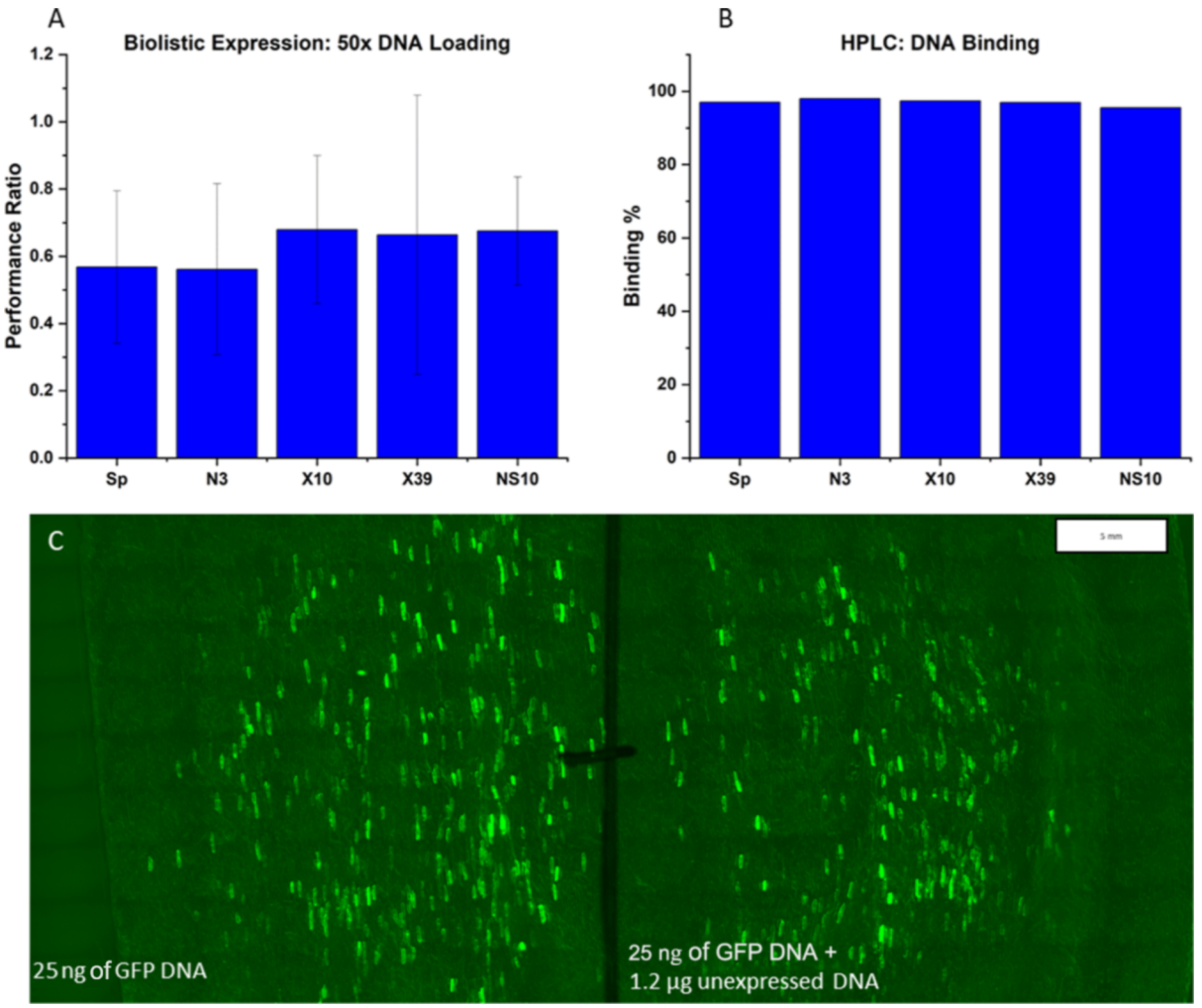

Figure 4. High-loading DNA delivery. Tests to determine the upper limit of DNA delivery for select library amines. (A) GFP-expressing DNA was diluted into other DNA and precipitated using one of a subset of amines as well as spermidine (Sp). Post bombardment, the number of fluorescent cells was compared to a non-diluted sample. (B) HPLC was also performed, with little variation evident between amines. The HPLC tests were performed using 50x the amount of DNA as the standard protocol (10 μg per batch). (C) This shows a representative image showing the captured image of a representative sample. The scale bar is 5 mm.

in the molecule's structure and performance. These descriptors provided thousands of unique quantitative data points associated with each molecule. These values are generated by QSAR modeling using existing data points to create models based purely on the structure that can be predictive of various properties such as melting point[26] or toxicity[32] (Figure 2B). The database offers a way to identify the factors that determine the trends in data in both biolistic and HPLC data.

The results showed a clear distinction between spermidine-like performance and ineffective amines (Figure 3). The biolistic data (Figure 3A) showed that all but a handful of amines demonstrated a performance ratio within a standard deviation of 1.0, which means that tested amines can deliver and express DNA similar to spermidine. The HPLC results (Figure 3B, which keeps amines in identical order to Figure 3A) show that most of the tested amines demonstrated near 100% DNA binding and 50−90% release efficiencies. Variance in the release data might be attributed to the lack of consistency in the test rather than the contribution of the structure as the assay involved multiple handling steps over the course of several hours.

The two sets are strongly correlated and together show a clear parity within the library. The correlation aligns well with the expected role of the amine in the delivery process: as a determining factor in the binding and release of the DNA. A more surprising result is the almost binary nature of the data set. All but a few amines fall within a similar range of *in vivo* and HPLC results. This suggests a lack of impact from many factors such as molecular weight or number of amines as these show no significant correlation within the results.

3.2. Descriptor Correlation and Amine Structure Analysis. Interestingly, five particular amines had distinctly poor performance (Figure 3D). Simply by looking at the structures, it becomes apparent that all molecules in this category contain oxygen. However, two other oxygen-containing amines are present elsewhere in the library (N7, X42) and show performance matching spermidine. Since both ethers and alcohols are present in both groups, specific functional groups are not likely the cause.

To try to identify any possible factor, we employed chemical descriptors to look for correlations that could also provide a functional explanation for the binding process. Using the Online Chemical Database with the modeling environment

https://doi.org/10.1021/acsabm.2c00689
ACS Appl. Bio Mater. XXXX, XXX, XXX−XXX

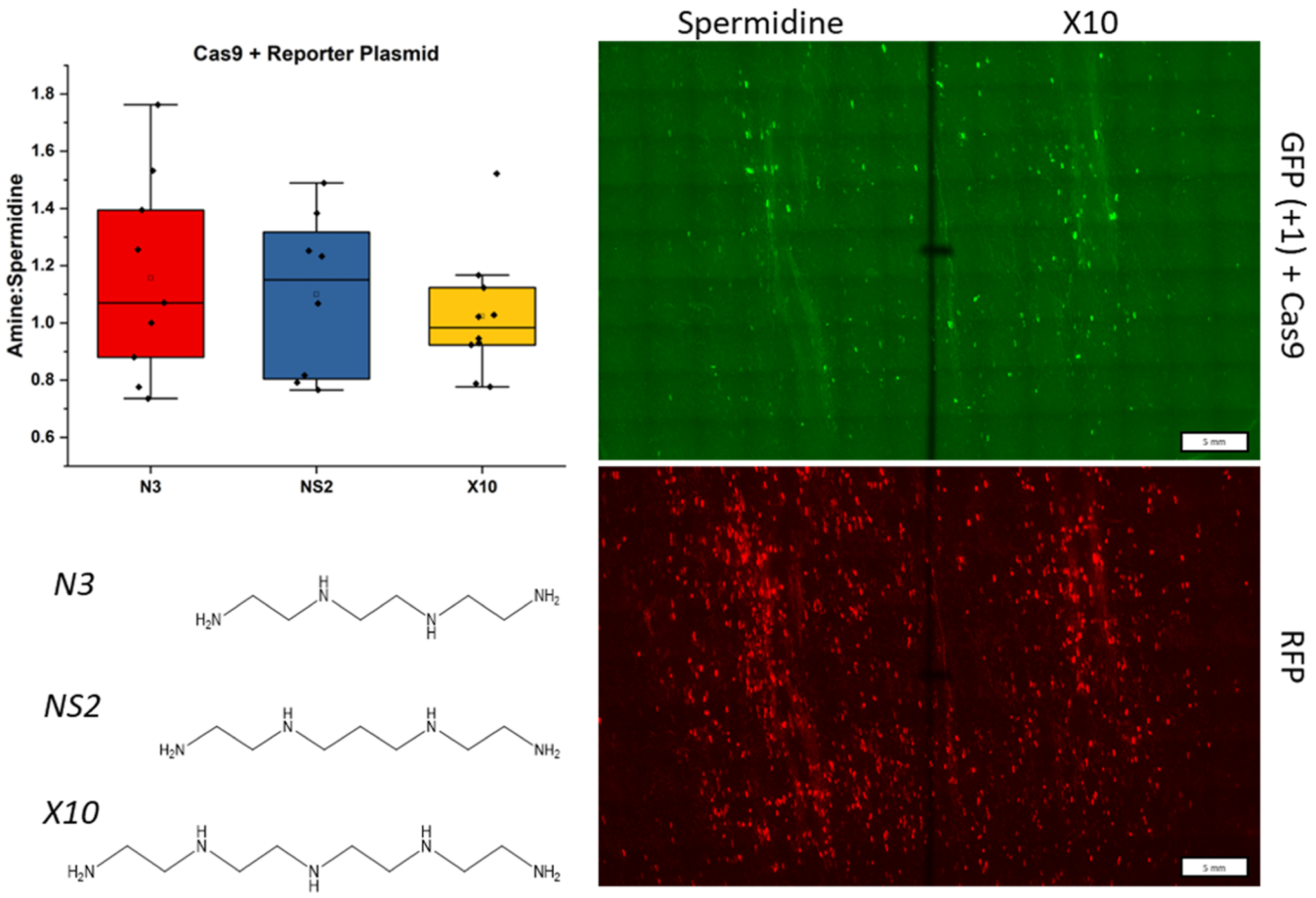

Figure 5. High DNA application. Three amines were selected to look for improvements in a novel system. A reporter plasmid encoding a gene for RFP expression as well as a frameshifted sequence for GFP expression was co-delivered with a plasmid encoded with Cas9 and gRNA to correct the frameshifted GFP. These plasmids were delivered in relatively high amounts (~10 μg total), and the results were compared to spermidine using the double-barrel system to ensure a consistent comparison. The scale bar is 5 mm.

(ochem.eu),[31] multiple descriptor models were employed to generate over 6000 unique descriptors. To remove noise from the analysis, these were correlated to the binary distribution of the results by giving the five poor performers a performance of 0 and the rest of the library as 1. The R^2 correlation value was determined for each descriptor, and only a handful of descriptors were significantly correlated (53/6221 descriptors had $R^2 > 0.6$). The most-correlated descriptors were almost entirely pH-modified versions of just a handful of descriptors: number of hydrogen bonds, number of hydrogen bond acceptors, and the energy of π-bonds within the molecule (Figure 3C, full list of top 20 are given in Supporting Table S2).

These descriptors suggest that the cause of poor performance is related to the overall charge of the molecule. All the highlighted descriptors are related to the presence of lone-pair electrons on atoms such as oxygen that do not protonate at the given pH (further explanation in the Supporting Information). These sources of negative charge disrupt the DNA−particle complexation that are encouraged by the positive charges on the protonated amine. When there are few lone pairs compared to the amines (N7, X10, X42), the delivery is successful. In the opposite situation, delivery is either diminished or completely prevented. Overall, these results emphasize the disruptive nature of negative charges in DNA−particle complexation as well as the corollary that practically any molecule containing only amine functional groups would be able to form a DNA−gold complex.

3.3. Delivery Efficiency of Higher DNA Amounts. An alternative explanation for the lack of distinction between the performance of the amines is that the DNA amounts used were too low to fully test the system. This is supported by the HPLC data, which indicate that ~100% of the DNA is bound in the precipitation. To test this, a subset of the library was re-examined using 50-fold more DNA, from 25 ng to 1.25 μg per shot, which is well above the amount used in other reported protocols (Figure 4A). Since GFP expression was already optimized at the lower DNA level, the amount of GFP-encoding plasmid was kept constant while another plasmid (pUC19) was added to increase the overall DNA amount. On the control side of the double barrel was the undiluted standard amount of GFP-encoding plasmid. While the number of GFP-expressing cells was slightly decreased (for many potential reasons) compared to the undiluted DNA (control side), the performance ratios remained remarkably consistent as shown in Figure 4A. Similar to the previous section, these amines were subjected to HPLC analysis of the binding, and the results indicated that very little DNA was left unbound during the DNA−gold complex formation (Figure 4B) despite the much larger amounts of DNA present.

To test a practical application of higher DNA amounts, we compared amines using a CRISPR-Cas9 editing system, in

https://doi.org/10.1021/acsabm.2c00689
ACS Appl. Bio Mater. XXXX, XXX, XXX−XXX

which a reporter plasmid was co-delivered with a Cas9-encoding editor plasmid.[22] Because of the need to capture the transient expression of the reporter and the editor, a large amount of both plasmids must be delivered, well over 1 μg per shot. The reporter plasmid pKL2187 carries an in-frame RFP gene as well as an out-of-frame GFP gene. The Cas9 construct encodes a single guide RNA (sgRNA) to target the out-of-frame leader of the GFP reporter gene, which leads to GFP production after successful editing. In this experiment, spermidine was compared to the selected amines. After bombardment and 48+ h of incubation at 30 °C, the numbers of cells expressing GFP and RFP were counted. The ratio of GFP (edited cells) to the RFP (total transfected cells) then provides a representation of the effectiveness or amount of Cas9 being expressed (Figure 5). The performance of the amine is then compared to the parallel delivery of the same reporter−editor system using spermidine, producing a similar performance ratio to the simple GFP expression experiments. The final results showed that each tested amine's performance remained within a standard deviation of the others. These results confirmed that the delivery capacity remains consistent between amines even at significantly higher DNA amounts. While it remains possible that they would differentiate at even higher amounts, it goes beyond the bounds of practicality. The consistency shown across different amine structures in both Figures 4 and 5 indicates that these amines are all able to bind the DNA equally well, despite changes in molecular weight, the bonding state of the amine group, the number of amine groups, or the molecular weight of the molecule.

4. CONCLUSIONS

In summary, the results of this study reveal the impact of amine selection on the delivery of DNA to plant tissues. Of the amines tested, the vast majority delivered as good as spermidine, the current standard. Analytical testing showed that the full amount of DNA was being bound to the gold, and this was true for almost all amines, even after increasing the amount of DNA 50-fold. This includes amines such as triethylamine, which is over an order of magnitude less expensive than spermidine. The increased DNA was also demonstrated with a Cas9 editing test that required a large amount of DNA to be delivered, and the end result was consistency between amine performance.

The chemical descriptors of the library were used to find the correlation between the few poor performers and their chemical properties. Several descriptors suggested that the presence of the lone electron pairs on the non-protonated functional groups was enough to disrupt the formation of the DNA−gold complex. This suggests that any molecule containing only amine functional groups would be able to perform at a similar level. The methods presented here can help understand the mechanism of biolistic delivery and improve the delivery of more challenging payloads, such as proteins in the future.

ASSOCIATED CONTENT

Supporting Information

The Supporting Information is available free of charge at https://pubs.acs.org/doi/10.1021/acsabm.2c00689.

Details on CellProfiler optimization, detailed explanation of descriptor definitions, tables showing the full amine list and top 20 correlated descriptors, and supporting figures such as the library structures, HPLC data comparing amine-less binding, double-barrel schematic, and amine toxicity results using fluorescence live−dead imaging (PDF)

AUTHOR INFORMATION

Corresponding Authors

Kan Wang − *Department of Agronomy and Crop Bioengineering Center, Iowa State University, Ames, Iowa 50011, United States*; Email: kanwang@iastate.edu

Shan Jiang − *Department of Materials Science and Engineering, Iowa State University, Ames, Iowa 50011, United States; Crop Bioengineering Center, Iowa State University, Ames, Iowa 50011, United States;* orcid.org/0000-0001-8119-9012; Email: sjiang1@iastate.edu

Authors

Kyle J. Miller − *Department of Materials Science and Engineering, Iowa State University, Ames, Iowa 50011, United States*

Connor Thorpe − *Department of Materials Science and Engineering, Iowa State University, Ames, Iowa 50011, United States*

Alan L. Eggenberger − *Department of Materials Science and Engineering, Iowa State University, Ames, Iowa 50011, United States; Crop Bioengineering Center, Iowa State University, Ames, Iowa 50011, United States;* orcid.org/0000-0002-8158-046X

Keunsub Lee − *Department of Agronomy and Crop Bioengineering Center, Iowa State University, Ames, Iowa 50011, United States*

Minjeong Kang − *Department of Agronomy, Crop Bioengineering Center, and Interdepartmental Plant Biology Major, Iowa State University, Ames, Iowa 50011, United States*

Fei Liu − *Department of Materials Science and Engineering, Iowa State University, Ames, Iowa 50011, United States*

Complete contact information is available at: https://pubs.acs.org/10.1021/acsabm.2c00689

Author Contributions

K.M.: Designed and conducted experiments, analyzed data, and wrote the manuscript. C.T.: Conducted experiments, analyzed data, and helped revise the manuscript. A.E.: Conducted experiments, analyzed data, and helped revise the manuscript. K.L.: Prepared DNA materials and helped revise the manuscript. M.K.: Conducted experiments, analyzed data, and helped revise the manuscript. F.L.: Conducted experiments, analyzed data, and helped revise the manuscript. S.J. and K.W.: Designed experiments, analyzed data, and helped revise the manuscript.

Notes

The authors declare no competing financial interest.

ACKNOWLEDGMENTS

This work was partially supported by the Agriculture and Food Research Initiative grant no. 2019-67013-29016 from the USDA National Institute of Food and Agriculture to S.J. and K.W., by the American Chemical Society Petroleum Research Fund under grant no. 60264-DNI7 and by 3M Non-tenured Faculty Award to S.J., by State of Iowa funds, by the seed grant fund from Crop Bioengineering Center of Iowa State

University to S.J., and by the USDA NIFA Hatch project #IOW04714, by State of Iowa funds. K.W.'s contribution to this work was partially supported by (while serving at) the National Science Foundation.

REFERENCES

(1) Ye, R.; Yang, X.; Rao, Y.; Basu, U.; Andras, C.; Ye, R.; Yang, X.; Rao, Y. Genetic Engineering Technologies for Improving Crop Yield and Quality. *Agronomy* **2022**, *12*, 759.
(2) John, M. E.; Agracetus, M. E. J. Cotton Crop Improvement Through Genetic Engineering. *Crit. Rev. Biotechnol.* **1997**, *17*, 185−208.
(3) Rai, M. K.; Shekhawat, N. S. Recent Advances in Genetic Engineering for Improvement of Fruit Crops. *Plant Cell Tissue Organ Cult.* **2014**, *116*, 1−15.
(4) Goldstein, D. A.; Thomas, J. A. Biopharmaceuticals Derived from Genetically Modified Plants. *QJM-An Int. J. Med.* **2004**, *97*, 705−716.
(5) Torney, F.; Moeller, L.; Scarpa, A.; Wang, K. Genetic Engineering Approaches to Improve Bioethanol Production from Maize. *Curr. Opin. Biotechnol.* **2007**, *18*, 193−199.
(6) Wang, K.; Frame, B. Biolistic Gun-Mediated Maize Genetic Transformation. *Methods Mol. Biol.* **2009**, *526*, 29−45.
(7) Fadeev, V. S.; Blinkova, O. V.; Gaponenko, A. K. Optimization of Biological and Physical Parameters for Biolistic Genetic Transformation of Common Wheat (Triticum aestivum L.) Using a Particle Inflow Gun. *Russ. J. Genet.* **2006**, *42*, 402−411.
(8) Sasaki, A.; Onoue, M.; Kanematsu, S.; Suzaki, K.; Miyanishi, M.; Suzuki, N.; Nuss, D. L.; Yoshida, K. Extending Chestnut Blight Hypovirus Host Range Within Diaporthales by Biolistic Delivery of Viral cDNA. *Mol. Plant Microbe Interact.* **2002**, *15*, 780−789.
(9) Banakar, R.; Schubert, M.; Collingwood, M.; Vakulskas, C.; Eggenberger, A. L.; Wang, K. Comparison of CRISPR-Cas9/Cas12a Ribonucleoprotein Complexes for Genome Editing Efficiency in the Rice Phytoene Desaturase (OsPDS) Gene. *Rice* **2020**, *13*, 4.
(10) Klein, T. M.; Gradziel, T.; Fromm, M. E.; Sanford, J. C. Factors Influencing Gene Delivery into Zea Mays Cells by High−Velocity Microprojectiles. *Bio/Technology* **1988**, *6*, 559−563.
(11) Ueki, S.; Lacroix, B.; Krichevsky, S.; Lazarowitz, V.; Citovsky, B. B.; Krichevsky, A.; Lazarowitz, S. G. Functional Transient Genetic Transformation of Arabidopsis Leaves by Biolistic Bombardment. *Nat Protoc* **2009**, *4* (1), 71−77.
(12) Parveez, G. K. A.; Chowdhury, M. K. U.; Saleh, N. M. Physical Parameters Affecting Transient GUS Gene Expression in Oil Palm (Elaeis guineensis Jacq.) Using the Biolistic Device. *Ind. Crops Prod.* **1997**, *6*, 41−50.
(13) Zilony, N.; Tzur-Balter, A.; Segal, E.; Shefi, O. Bombarding Cancer: Biolistic Delivery of Therapeutics Using Porous Si Carriers. *Sci. Rep.* **2013**, *3*, 1−6.
(14) Sawant, S. V.; Singh, P. K.; Tuli, R. Pretreatment of Microprojectiles to Improve the Delivery of DNA in Plant Transformation. *Biotechniques* **2000**, *29*, 246−248.
(15) Hamada, H.; Linghu, Q.; Nagira, Y.; Miki, R.; Taoka, N.; Imai, R. An in Planta Biolistic Method for Stable Wheat Transformation. *Sci. Rep.* **2017**, *7*, 11443.
(16) Sanford, J. C. The Biolistic Process. *Trends Biotechnol.* **1988**, *6*, 299−302.
(17) Sanford, J. C. Biolistic Plant Transformation. *Physiol. Plant.* **1990**, *79*, 206−209.
(18) Sudowe, S.; Reske-Kunz, A. B. *Biolistic DNA Delivery*, 1st ed.; Humana: Totowa, NJ, 2013.
(19) Green, J. J.; Langer, R.; Anderson, D. G. A Combinatorial Polymer Library Approach Yields Insight into Nonviral Gene Delivery. *Accounts Chem. Res.* **2008**, *41*, 749−759.
(20) Akinc, A.; Zumbuehl, A.; Goldberg, M.; Leshchiner, E. S.; Busini, V.; Hossain, N.; Bacallado, S. A.; Nguyen, D. N.; Fuller, J.; Alvarez, R.; Borodovsky, A.; Borland, T.; Constien, R.; de Fougerolles, A.; Dorkin, J. R.; Narayanannair Jayaprakash, K.; Jayaraman, M.; John, M.; Koteliansky, V.; Manoharan, M.; Nechev, L.; Qin, J.; Racie, T.; Raitcheva, D.; Rajeev, K. G.; Sah, D. W. Y.; Soutschek, J.; Toudjarska, I.; Vornlocher, H.-P.; Zimmermann, T. S.; Langer, R.; Anderson, D. G. A Combinatorial Library of Lipid-like Materials for Delivery of RNAi Therapeutics. *Nat. Biotechnol.* **2008**, *26*, 561−569.
(21) Vegas, A. J.; Veiseh, O.; Doloff, J. C.; Ma, M.; Tam, H. H.; Bratlie, K.; Li, J.; Bader, A. R.; Langan, E.; Olejnik, K.; Fenton, P.; Kang, J. W.; Hollister-Locke, J.; Bochenek, M. A.; Chiu, A.; Siebert, S.; Tang, K.; Jhunjhunwala, S.; Aresta-Dasilva, S.; Dholakia, N.; Thakrar, R.; Vietti, T.; Chen, M.; Cohen, J.; Siniakowicz, K.; Qi, M.; McGarrigle, J.; Graham, S.; Lyle, D. M.; Harlan, D. L.; Greiner, J.; Oberholzer, G. C.; Weir, R.; Langer, D. G.; Anderson, D. G. Combinatorial Hydrogel Library Enables Identification of Materials That Mitigate the Foreign Body Response in Primates. *Nat. Biotechnol.* **2016**, *34*, 345.
(22) Miller, K.; Eggenberger, A. L.; Lee, K.; Liu, F.; Kang, M.; Drent, M.; Ruba, A.; Kirscht, T.; Wang, K.; Jiang, S. An Improved Biolistic Delivery and Analysis Method for Evaluation of DNA and CRISPR-Cas Delivery Efficacy in Plant Tissue. *Sci. Rep.* **2021**, *11*, 11.
(23) McQuin, C.; Goodman, A.; Chernyshev, V.; Kamentsky, L.; Cimini, B. A.; Karhohs, K. W.; Doan, M.; Ding, L.; Rafelski, S. M.; Thirstrup, D.; Wiegraebe, W.; Singh, S.; Becker, T.; Caicedo, J. C.; Carpenter, A. E. CellProfiler 3.0: Next-Generation Image Processing for Biology. *PLoS Biol.* **2018**, *16*, No. e2005970.
(24) Speck-Planche, A.; Kleandrova, V. V.; Luan, F.; Cordeiro, M. N. D. S. Rational Drug Design for Anti-Cancer Chemotherapy: Multi-Target QSAR Models for the in Silico Discovery of Anti-Colorectal Cancer Agents. *Bioorg. Med. Chem.* **2012**, *20*, 4848−4855.
(25) Tropsha, A. Best Practices for QSAR Model Development, Validation, and Exploitation. *Mol. Inf.* **2010**, *29*, 476−488.
(26) Dearden, J. C. The QSAR Prediction of Melting Point, a Property of Environmental Relevance. *Sci. Total Environ.* **1991**, *109−110*, 59−68.
(27) Luke Mankin, S. L.; Thompson, W. F. New Green Fluorescent Protein Genes for Plant Transformation: Intron-Containing, {ER}-Localized, and Soluble-Modified. *Plant Mol. Biol. Rep.* **2001**, *19*, 13−26.
(28) Banakar, R.; Eggenberger, A. L.; Lee, K.; Wright, D. A.; Murugan, K.; Zarecor, S.; Lawrence-Dill, C. J.; Sashital, D. G.; Wang, K. High-Frequency Random DNA Insertions upon Co-Delivery of CRISPR-Cas9 Ribonucleoprotein and Selectable Marker Plasmid in Rice. *Sci. Rep.* **2019**, *9*, 19902.
(29) Kale, S. D.; Tyler, B. M. Assaying Effector Function in Planta Using Double-Barreled Particle Bombardment. *Methods Mol. Biol.* **2011**, *712*, 153−172.
(30) Dou, D.; Kale, S. D.; Wang, X.; Chen, Y.; Wang, Q.; Wang, X.; Jiang, R. H. Y.; Arredondo, F. D.; Anderson, R. G.; Thakur, P. B.; McDowell, J. M.; Wang, Y.; Tyler, B. M. Conserved C-Terminal Motifs Required for Avirulence and Suppression of Cell Death by Phytophthora Sojae Effector Avr1b. *Plant Cell* **2008**, *20*, 1118−1133.
(31) Sushko, I.; Novotarskyi, S.; Körner, R.; Pandey, A. K.; Rupp, M.; Teetz, W.; Brandmaier, S.; Abdelaziz, A.; Prokopenko, V. V.; Tanchuk, V. Y.; Todeschini, R.; Varnek, A.; Marcou, G.; Ertl, P.; Potemkin, V.; Grishina, M.; Gasteiger, J.; Schwab, C.; Baskin, I. I.; Palyulin, V. A.; Radchenko, E. V.; Welsh, W. J.; Kholodovych, V.; Chekmarev, D.; Cherkasov, A.; Aires-de-Sousa, J.; Zhang, Q. Y.; Bender, A.; Nigsch, F.; Patiny, L.; Williams, A.; Tkachenko, V.; Tetko, I. V. Online Chemical Modeling Environment (OCHEM): Web Platform for Data Storage, Model Development and Publishing of Chemical Information. *J. Comput. Aided Mol. Des.* **2011**, *25*, 533−554.
(32) Lagunin, A.; Zakharov, A.; Filimonov, D.; Poroikov, V. QSAR Modelling of Rat Acute Toxicity on the Basis of PASS Prediction. *Mol. Inf.* **2011**, *30*, 241−250.

https://doi.org/10.1021/acsabm.2c00689
ACS Appl. Bio Mater. XXXX, XXX, XXX−XXX